

We are IntechOpen, the world's leading publisher of Open Access books Built by scientists, for scientists

6,900

Open access books available

185,000

International authors and editors

200M

Downloads

Our authors are among the

154

Countries delivered to

TOP 1%

most cited scientists

12.2%

Contributors from top 500 universities



WEB OF SCIENCE™

Selection of our books indexed in the Book Citation Index
in Web of Science™ Core Collection (BKCI)

Interested in publishing with us?
Contact book.department@intechopen.com

Numbers displayed above are based on latest data collected.
For more information visit www.intechopen.com



Broadband Photodetectors Based on *c*-Axis Tilted Layered Cobalt Oxide Thin Films

Shufang Wang* and Guangsheng Fu

*Hebei Key Lab of Optic-Electronic Information and Materials, Hebei University, Baoding
PR China*

1. Introduction

Laser-induced voltage (LIV) effects in *c*-axis tilted thin films of YBa₂Cu₃O_{7-δ} (YBCO) and La_{1-x}Ca_xMnO₃ (LCMO) have been extensively studied in the past decades due to their potential applications in photodetectors [1-9]. Compared to the commonly used photodiodes-based photodetectors, this new type of photodetectors has the advantage of broad spectrum response ranging from ultra-violet (UV) to infrared (IR). Other advantages of this type of detectors consist in that they can be operated without cryogenic cooling and bias voltage.

The origin of the LIV signal was explained as result of the transverse thermoelectric effect which becomes effective when the *c* axis of YBCO or LCMO films are tilted by an angle α with respect to the film surface normal [8]. The induced voltage can be quantitatively described by the equation

$$U = \frac{l}{2d} \sin(2\alpha) \Delta S \Delta T \quad (1)$$

Where ΔT is the temperature difference between the top and bottom of the film, which is generated by heating the film surface due to the absorption of the incident laser radiation; $\Delta S = S_{ab} - S_c$ is the difference of the seebeck coefficient in the *ab*-plane and along the *c*-axis of the film; α is the tilted angle of the film with respect to the surface normal; d is the thickness of the tilted film and l is the laser spot diameter [1]. According to this equation, searching for materials having large anisotropy in seebeck coefficient, that is large ΔS , is a key factor for developing this new type photodetectors.

Recently, layered cobalt oxides including Na_xCoO₂, Ca₃Co₄O₉, Bi₂Sr₂Co₂O_y and etc. have attracted great attention as promising thermoelectric materials due to their good thermoelectric performance as well as the good thermal stability, lack of sensitivity to the air and non-toxicity [10-14]. The crystal structure of these cobalt oxides consists of the conducting CoO₂ layer and the insulating Na, Ca₂CoO₃ or Bi₂Sr₂O₄ layer, which are alternately stacked along the *c*-axis. This layered structure results in a large anisotropy of the

* Corresponding Author

seebeck coefficient in the *ab*-plane and along the *c*-axis of the film, realizing $\Delta S = S_{ab} - S_c$ of tens of $\mu\text{V/K}$, which is about several times larger than that of YBCO ($\sim 10 \mu\text{V/K}$) and hundreds times larger than that of LCMO ($\sim 0.22 \mu\text{V/K}$) [3, 4]. This fact indicates the layered cobalt oxides might have potential applications in the field of high-sensitive broadband photodetectors. In this chapter, we present our investigation of LIV effects in *c*-axis tilted cobalt oxide thin films (Na_xCoO_2 , $\text{Ca}_3\text{Co}_4\text{O}_9$ and $\text{Bi}_2\text{Sr}_2\text{Co}_2\text{O}_y$) with different pulsed laser sources with wavelength ranging from UV to NIR. The open-circuit voltage signals were detected in these films when their surfaces were irradiated by the laser light. The results demonstrate that the *c*-axis tilted cobalt oxide thin films have great potential applications in the broadband photodetectors.

2. Sample preparation and LIV measurements

2.1 Fabrication of *c*-axis tilted Na_xCoO_2 , $\text{Ca}_3\text{Co}_4\text{O}_9$ and $\text{Bi}_2\text{Sr}_2\text{Co}_2\text{O}_y$ thin films

The *c*-axis inclined Na_xCoO_2 thin film was obtained by epitaxially growing a layer of Na_xCoO_2 ($x \sim 0.7$) on a tilted Al_2O_3 (0001) single crystal substrate by topotaxially converting an epitaxial CoO film to Na_xCoO_2 with annealing in Na vapor. A CoO film was first epitaxial grown on the tilted Al_2O_3 (0001) by pulsed laser deposition. The CoO film was then sealed in an alumina crucible with NaHCO_3 powder and heated to 700–750°C for 60 min to form the Na_xCoO_2 film. The *c*-axis tilted $\text{Ca}_3\text{Co}_4\text{O}_9$ and $\text{Bi}_2\text{Sr}_2\text{Co}_2\text{O}_y$ thin films can be grown on the tilted LaAlO_3 (001) or Al_2O_3 (0001) substrates with the pulsed laser deposition (PLD) or chemical solution deposition (CSD) methods. The detailed PLD and CSD fabrication parameters can be found in Ref. 15–17. Transport measurements on these films reveal that they have the room temperature seebeck coefficient comparable to that of the single crystals, suggesting good quality of these films.

Fig. 1a–c presents the x-ray diffraction (XRD) θ - 2θ scans of the *c*-axis tilted cobalt oxide thin films on 10° tilted substrates. The offset angle ω is the angle between the *c*-axis direction and the substrate surface-normal direction and it is set as 10° (See the inset of Fig. 1a). Apart from the substrate peak, all peaks in these patterns can be indexed to the (00 l) diffractions of the corresponding layered cobalt oxides, indicating that phase-pure *c*-axis tilted Na_xCoO_2 , $\text{Ca}_3\text{Co}_4\text{O}_9$ and $\text{Bi}_2\text{Sr}_2\text{Co}_2\text{O}_y$ thin films are obtained and the tilted angle is 10°.

2.2 LIV measurements

Fig. 2 presents the schematic illustration of the LIV measurements. Two indium or gold electrodes with the diameter of ~ 0.4 mm were symmetrically deposited on the film surface along the inclined direction and they were separated by 4 mm. To prevent the generation of any electric contact effect, the electrodes were always kept in the dark. A XeCl excimer pulsed laser ($\lambda = 308$ nm, $t_p \sim 20$ ns) and an Nd:YAG pulsed laser ($\lambda = 532$ and 1064 nm, $t_p \sim 25$ ps) were used as the light sources. The incident laser beam, adjusting to 2 mm in diameter using an aperture, was directed perpendicular to the film surface at the middle position between the two electrodes. The induced lateral voltage signals were recorded using a digital oscilloscope of 500 MHz bandwidth terminated into 1 M Ω (Tektronix, TDS 3052).

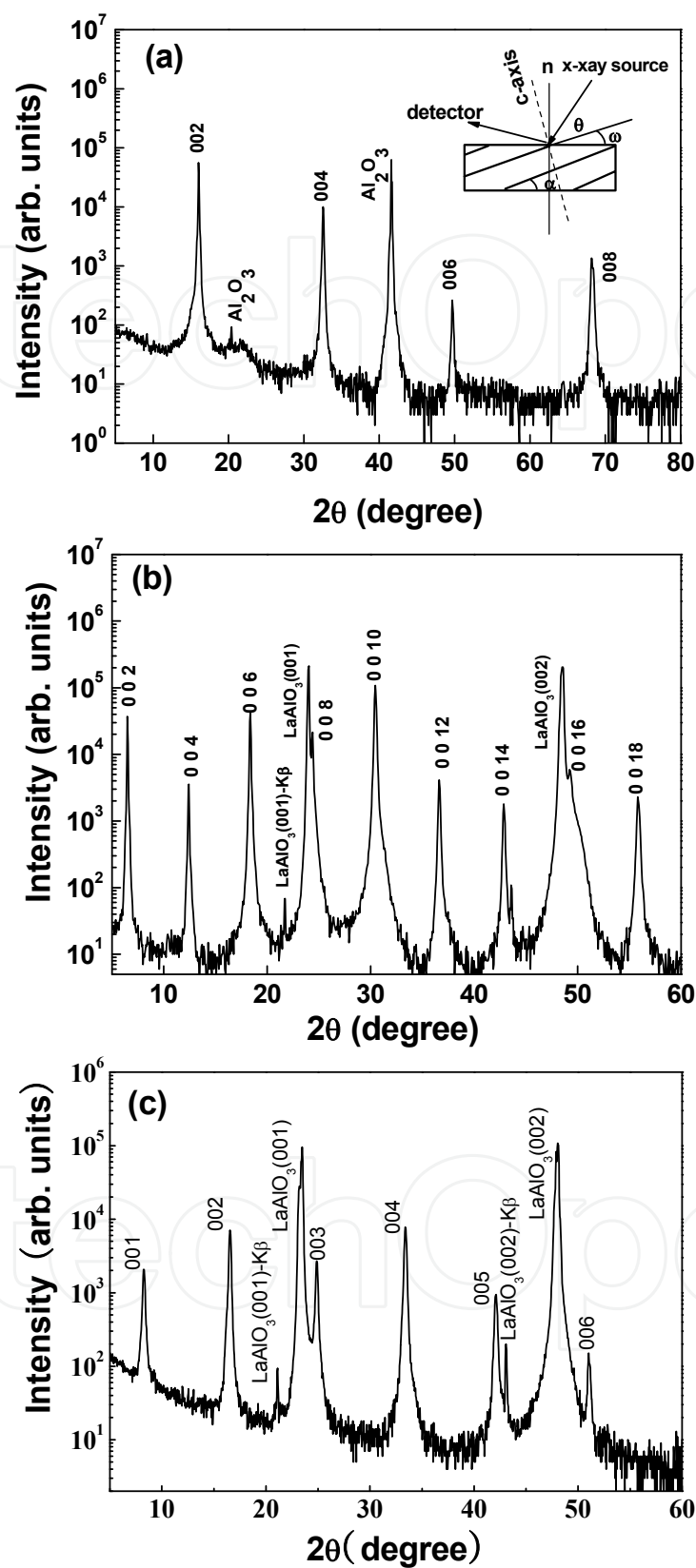


Fig. 1. XRD θ - 2θ scans for the *c*-axis tilted (a) Na_xCoO_2 , (b) $\text{Bi}_2\text{Sr}_2\text{Co}_2\text{O}_y$ and (c) $\text{Ca}_3\text{Co}_4\text{O}_9$ thin film on 10° tilted single crystal substrates. The inset of Fig. 1a is the sketch map of the XRD θ - 2θ measurement and the offset angle ω is set as 10° .

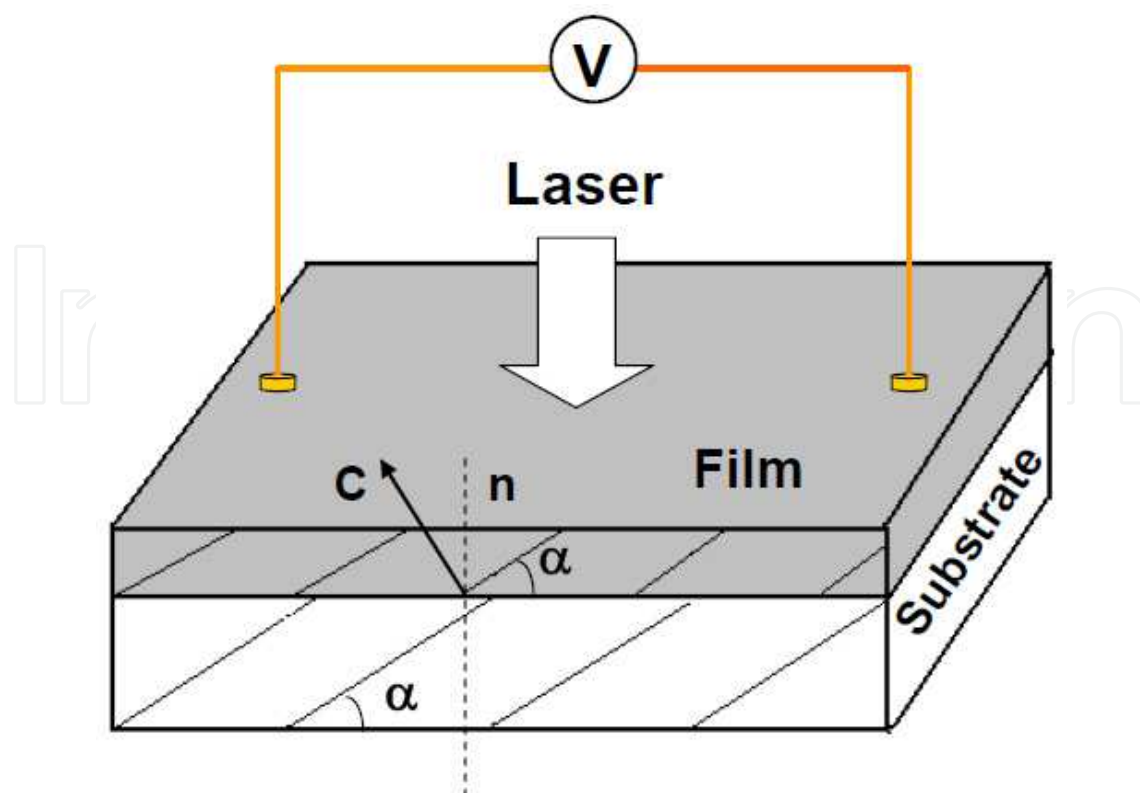


Fig. 2. Schematic illustration of the LIV measurements.

3. Results and discussion

3.1 LIV response of the c-axis tilted $\text{Bi}_2\text{Sr}_2\text{Co}_2\text{O}_y$ thin films to different laser pulses

Fig. 3a-c presents the response of a 10° tilted $\text{Bi}_2\text{Sr}_2\text{Co}_2\text{O}_y$ thin film (~ 100 nm) to the laser pulses of 308 nm, 532 nm and 1064 nm, respectively. Large open-circuit signals with the response time in the order of several hundred nanoseconds are detected for these three wavelengths. The voltage responsivity is calculated to be about 440 mV/mJ, 348 mV/mJ and 65 mV/mJ for 308 nm, 532 nm and 1064 nm pulsed radiations respectively. The stronger LIV signals obtained for the UV 308 nm and visible 532 nm lasers than that for the NIR 1064 nm laser can be explained by considering the different optical absorption and penetration depth of the radiations with different wavelength in $\text{Bi}_2\text{Sr}_2\text{Co}_2\text{O}_y$ film. The higher absorption and smaller penetration depth of 308 nm and 532 nm radiation in comparison with these of the 1064 nm radiation lead to a larger ΔT and thus a larger induced voltage.

To reduce the influence of the RC measurement circuit on the response time, a $2\ \Omega$ load resistance is connected parallel with the tilted film while keeping other experimental conditions unchanged. As shown in Fig. 4, the rise time is dramatically decreased from 100 ns shown in Fig. 2a to about 6 ns and the FWHM is also decreased from 470 ns to be about 20 ns. It should be mentioned here that the response time has a pronounced dependence on the pulse width of the incident lasers. The smaller pulse width usually leads to a faster response time. For example, the FWHM of the induced voltage signal is reduced to 1-2 ns when the same film is irradiated by the Nd:YAG picosecond laser pulse. The nanosecond-scale response of the tilted $\text{Bi}_2\text{Sr}_2\text{Co}_2\text{O}_y$ thin film to different laser pulses ranging from UV to NIR reveals that it has a potential application in broadband photodetectors with fast response.

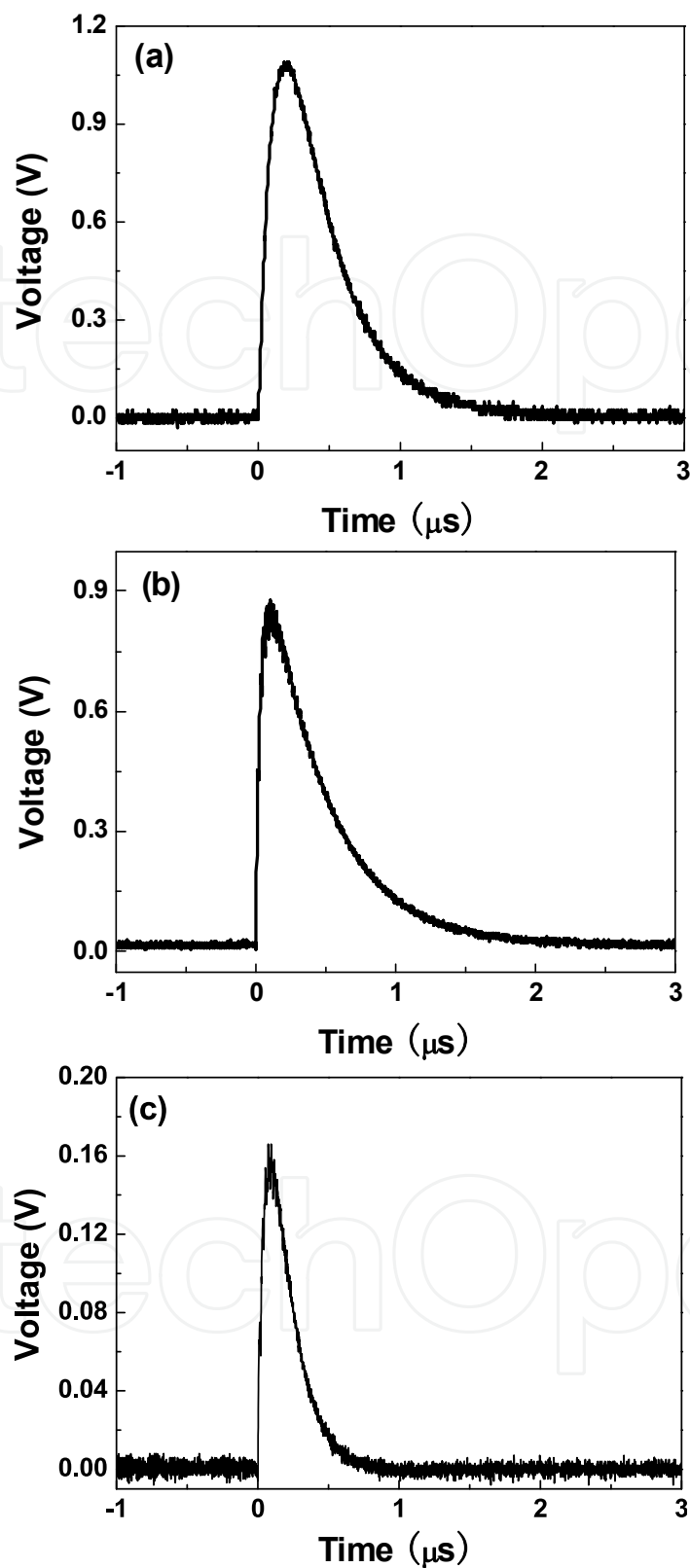


Fig. 3. LIV signals of a 10° *c*-axis tilted Bi₂Sr₂Co₂O_y thin film (~ 100 nm) when its surface is irradiated by the pulsed lasers with different wavelength of (a) 308 nm, (b) 532 nm and (c) 1064 nm. The input impedance of an oscilloscope is 1 M Ω and the laser energy on the sample is about 2.5 mJ.

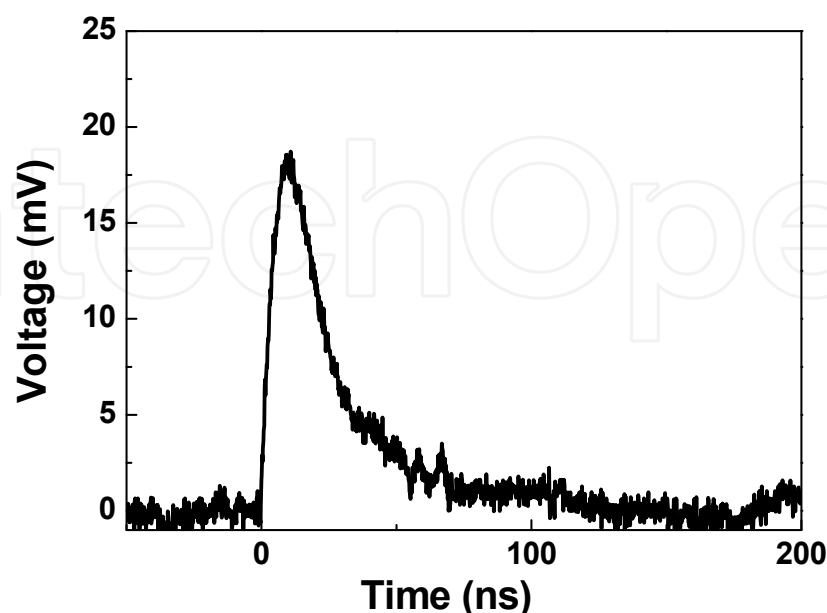


Fig. 4. LIV signal of a 10° *c*-axis tilted $\text{Bi}_2\text{Sr}_2\text{Co}_2\text{O}_y$ thin film under the 308 nm radiation after connecting a $2\ \Omega$ load resistance in parallel with the tilted film.

3.2 Dependence of the peak voltage of the LIV response on the laser energy, tilted angle and film thickness

Fig. 5a shows the dependence of the peak value of the open-circuit voltage signal (V_p) in the tilted $\text{Bi}_2\text{Sr}_2\text{Co}_2\text{O}_y$ thin film on the 308 nm laser energy on the film surface. A linear dependence is obtained for laser energy below the destruction limit of the film. The dependence of the LIV signal of the tilted $\text{Bi}_2\text{Sr}_2\text{Co}_2\text{O}_y$ film on the tilted angle α is also investigated and an almost linear relationship between the V_p value and α is obtained, seen in Fig. 5b. This $U \propto \sin 2\alpha$ dependence again demonstrates that the LIV effect in the *c*-axis tilted layered cobalt oxides thin films mainly originates from the transverse thermoelectric effect since all other light-induced effects do not shown such tilt angle dependence.

Fig. 5c presents V_p as a function of the film thickness under 308 nm laser radiation. The V_p increases with the decrease of film thickness and reaches a maximum value when the film thickness is about 100 nm, and then V_p turns to a reduction with further decreasing film thickness from 100 nm to 60 nm. This is inconsistent with Eq. (1) where V_p increases monotonically with decreasing d . Similar V_p - d dependence was observed in the LIV measurements for *c*-axis tilted YBCO and LCMO films. An improved equation based on the plane heat source and cascade power net model was proposed to explain this abnormal behavior. Calculations based on this improved equation revealed that V_p was no more monotonic variation with the thickness d and there existed an optimum thickness corresponding to a maximum peak of the induced signal [9].

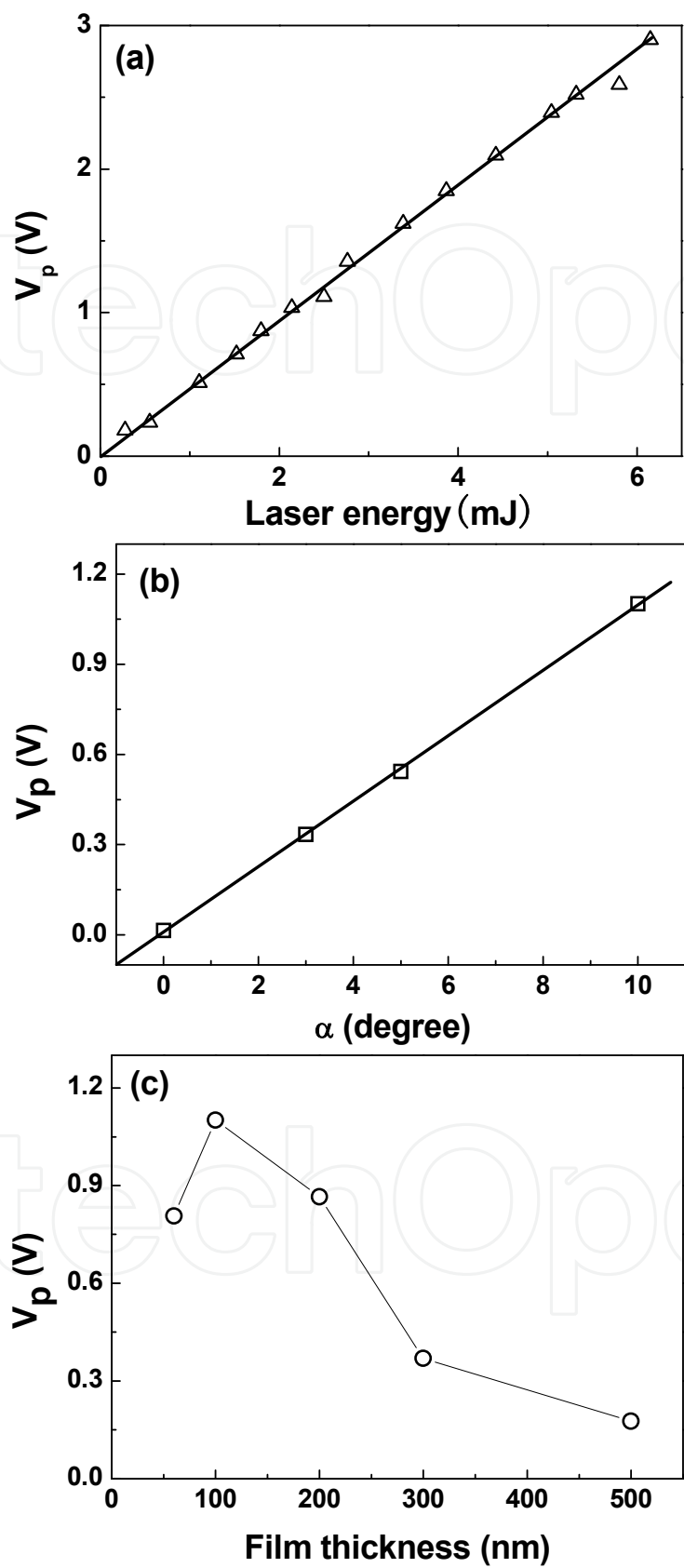


Fig. 5. Dependence of the peak value of the induced open-circuit voltage (V_p) on the (a) laser energy on the film surface, (b) tilted angle α and (c) film thickness. Solid lines are guide for eyes.

3.3 LIV signal in *c*-axis $\text{Ca}_3\text{Co}_4\text{O}_9$ and Na_xCoO_2 thin films

Similar results are also observed in the *c*-axis tilted $\text{Ca}_3\text{Co}_4\text{O}_9$ thin films when their surface is irradiated by the above lasers. Fig. 6 presents a typical laser-induced open-circuit voltage signal of the 10° tilted $\text{Ca}_3\text{Co}_4\text{O}_9$ thin film ($\sim 100\text{ nm}$) under the 308 nm pulsed illumination with the laser energy on the sample of 1 mJ . Both the responsivity ($\sim 230\text{ mV/mJ}$) and the response time (the rise time $\sim 60\text{ ns}$ and the FWHM $\sim 700\text{ ns}$) of the LIV signal in this tilted $\text{Ca}_3\text{Co}_4\text{O}_9$ thin film is in the same order as that of the tilted $\text{Bi}_2\text{Sr}_2\text{Co}_2\text{O}_y$ thin film with the same thickness.

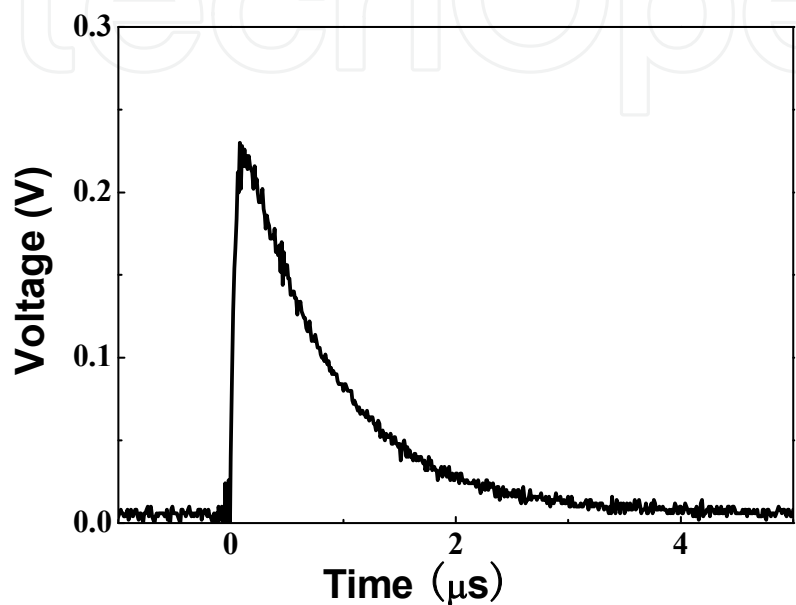


Fig. 6. A typical LIV signal of a 10° *c*-axis tilted $\text{Ca}_3\text{Co}_4\text{O}_9$ thin film ($\sim 100\text{ nm}$) under the 308 nm laser radiation. The laser energy on the sample is about 1 mJ .

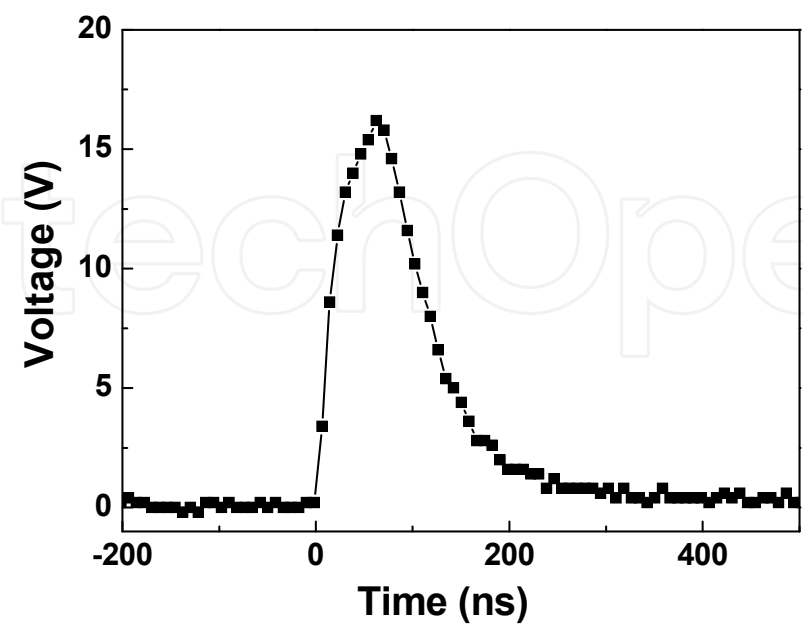


Fig. 7. A typical LIV signal of a 10° *c*-axis tilted Na_xCoO_2 thin film ($\sim 140\text{ nm}$) under the 308 nm laser radiation. The laser energy on the sample is about 1.5 mJ .

The performed LIV measurements on the *c*-axis tilted Na_xCoO_2 thin films show similar dependence of V_p on the laser energy, tilted angle α and film thickness. However, the *c*-axis tilted Na_xCoO_2 thin films have a much larger induced voltage signal than that of the $\text{Bi}_2\text{Sr}_2\text{Co}_2\text{O}_y$ and $\text{Ca}_3\text{Co}_4\text{O}_9$ thin films. Fig. 7 illustrates the laser-induced open-circuit voltage signal of the 10° tilted Na_xCoO_2 film irradiated by the 308 nm pulsed laser with the laser energy on the sample of 1.5 mJ. A giant open-circuit voltage signal with V_p of 16.3 V is observed. The responsivity is calculated to be about 11 V/mJ. It is much larger than the responsivity of YBCO, LCMO and other two cobalt oxide thin films [1-4, 18, 19]. This might be due to the Na_xCoO_2 film has better crystal quality which corresponds to a larger ΔS , and the exact reason needs to be clarified in our future work.

4. Conclusion

In conclusion, the performed investigations of the LIV effect in *c*-axis tilted Na_xCoO_2 , $\text{Bi}_2\text{Sr}_2\text{Co}_2\text{O}_y$ and $\text{Ca}_3\text{Co}_4\text{O}_9$ thin films at room temperature show that large open-circuit lateral voltage signals with the rise time in the order of several nanoseconds are measured when the surface of these films is irradiated by different laser sources with the wavelength ranging from UV to NIR. The obtained results suggest that *c*-axis tilted cobalt oxide thin films can be used for broadband photodetectors with fast response.

5. Acknowledgments

This work was partially supported by NSFC of China under Grant No. 10904030, SFC of Hebei Province under Grant No. A2009000144 and E 2006001006.

6. References

- [1] H. Lengfellner, G. Kremb, A. Schnellbbgl, J. Betz, K. F. Renk, W. Prettl, Appl. Phys. Lett. 60, 601(1992)
- [2] S. Zeuner, W. Prettl, H. Lengfellner, Appl. Phys. Lett. 66, 1833 (1995)
- [3] Th. Zahner, R. Stierstorfer, S. Reindl, T. Schauer, A. Penzkofer, H. Lengfellner, Physica C 313, 37(1999)
- [4] P.X. Zhang, W.K. Lee, G.Y. Zhang, Appl. Phys. Lett. 81, 4026(2002)
- [5] H.-U. Habermeiera, X.H. Li, P.X. Zhang, B. Leibold, Sol. State Commun. 110, 473(1999)
- [6] K. Zhao, M. He, G.Z. Liu, H.B. Lu, J. Phys. D: Appl. Phys. 40, 5703(2007)
- [7] S. Zeuner, H. Lengfellner, W. Prettl, Phy. Rev. B 51, 11903 (1995)
- [8] H. Lengfellner, S. Zeuner, W. Prettl, K. F. Renk, Europhys. Lett. 25, 375 (1994)
- [9] P.X. Zhang and H.-U. Habermeier, J. Nanometers 2008, 329601 (2008)
- [10] I. Terasaki, Y. Sasago, K. Uchinokura, Phys. Rev. B 56, R12685(1997)
- [11] Y.Y. Wang, N.S. Rogado, R.J. Cava, N.P. Ong, Nature (London) 423, 425 (2003)
- [12] M. Shikanoa, R. Funahashi, Appl. Phys. Lett. 82, 1857(2003)
- [13] R. Funahashia, M. Shikano, Appl. Phys. Lett. 81, 1459(2001)
- [14] K. Koumoto, I. Terasaki, R. Funahashi, MRS Bulletin 31, 206 (2006)
- [15] S.F. Wang, Z.C. Zhang, L.P. He, M.J. Chen, W. Yu, G.S. Fu, Appl. Phys. Lett. 94, 162108 (2009)
- [16] S.F. Wang, A. Venimadhav, S.M. Guo, K. Chen, X. X. Xi, Appl. Phys. Lett. 94, 022110 (2009)

- [17] S.F. Wang, M.J. Cheng, L.P. He, W. Yu, G.S. Fu, J. Phys. D: Appl. Phys. 42, 045410 (2009)
- [18] S.F. Wang, J.C. Chen, X.H. Zhao, S.Q. Zhao, L.P. He, M.J. Chen, W. Yu, J.L. Wang, G.S. Fu, Appl. Sur. Sci. 257, 157(2010)
- [19] S.F. Wang, J.C. Chen, S.R. Zhao, L.P. He, M.J. Chen, W. Yu, J.L. Wang, G.S. Fu, Chin. Phys. B 19, 107201 (2010)

IntechOpen

IntechOpen



Photodetectors

Edited by Dr. Sanka Gateva

ISBN 978-953-51-0358-5

Hard cover, 460 pages

Publisher InTech

Published online 23, March, 2012

Published in print edition March, 2012

In this book some recent advances in development of photodetectors and photodetection systems for specific applications are included. In the first section of the book nine different types of photodetectors and their characteristics are presented. Next, some theoretical aspects and simulations are discussed. The last eight chapters are devoted to the development of photodetection systems for imaging, particle size analysis, transfers of time, measurement of vibrations, magnetic field, polarization of light, and particle energy. The book is addressed to students, engineers, and researchers working in the field of photonics and advanced technologies.

How to reference

In order to correctly reference this scholarly work, feel free to copy and paste the following:

Shufang Wang and Guangsheng Fu (2012). Broadband Photodetectors Based on c-Axis Tilted Layered Cobalt Oxide Thin Films, Photodetectors, Dr. Sanka Gateva (Ed.), ISBN: 978-953-51-0358-5, InTech, Available from: <http://www.intechopen.com/books/photodetectors/broadband-photodetectors-based-on-c-axis-tilted-layered-cobalt-oxide-thin-films->

INTech
open science | open minds

InTech Europe

University Campus STeP Ri
Slavka Krautzeka 83/A
51000 Rijeka, Croatia
Phone: +385 (51) 770 447
Fax: +385 (51) 686 166
www.intechopen.com

InTech China

Unit 405, Office Block, Hotel Equatorial Shanghai
No.65, Yan An Road (West), Shanghai, 200040, China
中国上海市延安西路65号上海国际贵都大饭店办公楼405单元
Phone: +86-21-62489820
Fax: +86-21-62489821

© 2012 The Author(s). Licensee IntechOpen. This is an open access article distributed under the terms of the [Creative Commons Attribution 3.0 License](#), which permits unrestricted use, distribution, and reproduction in any medium, provided the original work is properly cited.

IntechOpen

IntechOpen